International Journal of Engineering and Advanced Technology (IJEAT)
ISSN: 2249-8958 (Online), Volume-8 Issue-2S, December 2018

Detection of Malignant Skin Disease Based on Lesion Segmentation – A Survey

Kailas Tambe, G. Krishna Mohan

Abstract--- The scope of the project is diagnosis the malignancy of skin disease using digital camera images. Melanoma, a kind of skin disease predominantly distributed amongst 25% of population. If melanoma is detected in its early stage the chances of recovery and medication of diseases are higher. Though dermascopy, a non-invasive skin imaging technique gives a possible solution for accurate screening yet cost of screening is high hence an automated system for diagnosis is required. The image of skin lesion is captured by digital camera using which locating the skin lesion is another challenge of segmenting the vulnerable or affected area from the normal region. To increase the sensitivity and precision of diagnosis skin lesion segmentation algorithm based on texture based is reviewed. Segmentation is performed for accurate detection of lesion and texture distributions are analyzed with illumination corrected image followed by calculating the texture distinctiveness metrics. The prediction of texture distributions in the image can be classified into melanoma or normal skin. The validation of results is done using MATLAB 2017b software.

Keywords— Dermascopy, skin lesion segmentation algorithm, texture distinctiveness

I. INTRODUCTION

Melanoma is a kind of skin cancer caused in accordance to prolonged exposure to ultraviolet light rays. The pigment containing cells are known as melanocytes. Under most of the circumstances melanoma might develop from a mole that can be identified with the size of the pigmented region expanding in its size, edges are not having improper shaped edges, difference in color, itchiness, or breakdown of skin. Benign and malignant tumors are categorized under pigmented skin lesion wherein moles are benign and melanoma is of malignant and is one of the severe types of cancers. The most common diagnostic technique is visual inspection of candidates, which are abnormal shaped and colored moles. In order for early diagnosis of melanomas 'ABCDE' rule [1] is applied to examine moles for malignancy. Even then the differentiation of the malignant cells from non-malignant conditions is cumbersome and poses challenges to the dermatologists under certain situations. Acquisition of images using digital dermatoscope performs the task of a filter as well as magnifier by early automation in screening melanoma. Such acquired dermascopy images has low levels of noise but consistent illumination at the background and their accuracy of detection can be increased with automated melanoma screening algorithms compared to a standard digital camera.

A. Abcde method

The familiar method for understanding and predicting the indicators of melanoma is 'ABCDE' rule:

1. Asymmetrical skin lesion
2. Border of the lesion is aberrant
3. Color of melanomas
4. Diameter of moles greater than 6 mm are more likely to be melanomas
5. Enlarging or evolving

But unfortunately most of the melanomas have diameter comparatively below the range of 6 mm and they appear as a dot. There are even chances of false alarms during seborrheic keratosis on following the ABCD criteria and needs to be examined by doctors for distinguishing seborrheic keratosis from melanoma with dermatoscopy. Nodular melanoma has to be classified using EFG as it does not fall into the above mentioned criteria's:

1. Elevated: the lesion is raised above the surrounding skin
2. Firm: the nodule is hard when touched
3. Growing: the nodule gradually increases in size

The validation and estimation of chromatic and structural parameters using decision-tree classification techniques for the application in specific images collected from MIT database on skin lesion are carried out using processing algorithms. Decision Tree Classifier being one of the prominent machine learning algorithms has been utilized for suitably classifying the pigmented network of the skin lesion [2] along with multistage illumination algorithm for variation in images of skin lesion [3]. The computation of the illumination map for photograph using Monte Carlo non-parametric modeling is a preliminary strategy followed by estimation of the illumination map where the initial nonparametric estimate is used as a prior via a parametric modeling. The final illumination map estimate is obtained from processed photograph. Textural representations based extraction in defining the image in sparse texture model using Rotational-invariant neighborhood is analyzed [3]. Weighted graphical modeling for the features extracted by sparse texture model is characterized for the statistical [4] textural distinctiveness among representative atom pairs and are computed from the frequency of occurrence across each pixel at a time.

Manuscript published on 30 December 2018.
***** Correspondence Author (s)
Kailas Tam, Department of Electronics and Communication Engineering, Bannari Amman Institute of Technology, Sathyamangalam, Erode, Tamil Nadu, India (prettz_d@yahoo.in)
Dr. G. Krishna Mohan, Department of Electronics and Communication Engineering, Bannari Amman Institute of Technology, Sathyamangalam, Erode, Tamil Nadu, India (baranidhar@hotmail.com)

At each pixel level, the stochastic region merging is performed to segment the regions corresponding to skin lesions from the macroscopic images [1] and subsequently on a region until the limit of convergence condition is attained. The foremost likelihood function used for merging up of regions in a stochastic manner is regional statistics. The machine learning approach [4] is adapted owing to the nature of automatic quantification of certain frequency of colors in dermascopy images. With the given 'N' true-color composited dermascopy image, reducing their number of colors lesser than required using K-means clustering algorithm is incorporated i.e., K<<N, where K is spatial term and its optimal value is estimated using cluster validity. The cluster output of the derived function is then thresholded to estimate the diagnosis between benign or malignant of the input image.

The Bag-of-Features approach [5] for detection of can be sort out in either of two ways such as histogram representation or identification of clusters using training set. The quantitative representation of an image in three channel method requires pre-processing, in segmentation and features extracted for lesion generated for lesion classification. Though there are various classifiers involved in image segmentation, prominent results are achieved using Naive Bayes and Support Vector Machine. Also enhanced TDLS algorithm [5] and SVM classifier provides automated pre-screening for diagnosing melanoma. Texture distributions are derived from texture vectors without probabilistic information. The method will segment the images of skin cancer and other pigmented lesions automatically. To classify between the two different classes of melanoma, extracting the features based on Gray Level Co-occurrence matrix (GLCM) and Multilayer Perceptron classifier (MLP) are often preferred.

In section II a brief review about the existing technique is discussed followed by the proposed work in section III where the implementation of automated texture based algorithm is discussed. The section IV entails upon the simulation results and analysis and in section V, the entire work is being reviewed and concluded.

II. EXISTING METHODOLOGIES

In the existing system the malignant skin lesion is detected using the following method even with the environmental disturbances.

A. Border detection

The gray scale image is extracted from RGB image using median filter and contrast enhancement. Fig.1 shows the color image and are then segmented using the active contour method with continuous maximal separation of background disturbance using the preprocessing methods [6]. This method is also known as snake method. Chan-Vese model of active contouring is implemented as it is comparatively a better algorithm on energy minimization problem. In addition this method requires the initialization of a curve or binary mask of square, circle or rectangle. Under each iteration, the shape moves to minimize the energy function [7].

Fig.1 The color image followed by segmented image using the active contour method

B. Features of the lesion

As discussed previously the common features that are predominantly considered for diagnosing skin lesions are Asymmetry, Border irregularity, Color variation and Diameter in short called as 'ABCD' rule.

B.1 Asymmetry

Since the malignant lesions do not have a symmetric appearance, a key parameter in detecting lesion a best fit ellipse is considered in obtaining the segmentation inside the lesion and splitting into equal halves along its major axis and they are then overlapped in order to check the symmetry of the lesion.

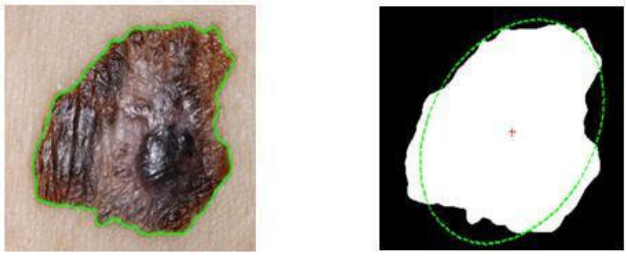

Fig.2 The color image followed by segmented image showing the best fit ellipse to trace the symmetry

B.2 Border irregularity

On comparing the smoothness border function of the infection skin, the benign and other normal skin lesions with which distinction is actually done has thin circumference. This irregularity in border can be determined by CI [Compactness Index] as in equation (1):

$$CI = \frac{P^2}{4A} \qquad \text{.....(1)}$$

where P and A are perimeter and area of the segmented lesion [8]. For a symmetric circle, CI has to be 1 and increases gradually as size increases. In addition to CI, Border irregularity is yet another prominent parameter that describes a smooth or rugged border of the lesion. This was determined using the compactness index value where the value increases as the ruggedness of the border increases. The compactness index value was calculated and was found that the malignant lesions varied over a range of l.80 to 2.95 with eight exception cases with the range of non-malignant is from 1.53 to 1.71

Published By:
Blue Eyes Intelligence Engineering
and Sciences Publication (BEIESP)

B.3 Color variation

Malignant lesions are often colored and it obviously will include primitive colors like red, black, light brown and white unlike non-malignant. As the channels constitutes of three colored images, the variation of color in the lesion can be achieved by using normalized standard deviation combining all three channels by the given equation (2):

$$C_{r,g,b} = {}^{r,g,b}{}_{M}\, r, g, b \quad \ldots\ldots\ldots (2)$$

where C and r, g, b represents values of three color variation in each channel and standard deviations of channel r,g,b

such as red, green and blue respectively with the maximum values of each color channels is denoted by M r,g,b. The color variations Cr,g,b are independently determined for each segment separately. For a colored lesion, the variation

would be large whereas for a uniformly colored lesion, it would show a minor variation for the two halves which isI once again analyzed by dividing the lesion into two halves along its major axis as discussed earlier.

B.4 Diameter of the lesion

Diameter is one of the simplest and traditional methods in predicting whether the segment is malignant or not just by considering the length of the major axis in best fit ellipse. A lesion is considered as malignant if the diameter is about 6mm or more since these lesions grows bigger than the non-malignant lesions and this conclusion is arrived based on aforementioned ABCD rule. Therefore, this is a key parameter that clearly distinguishes the malignancy based on the lesion's diameter.

III. PROPOSED METHODOLOGY

The proposed framework based on texture distinctiveness lesion segmentation [9] shows higher segmentation accuracy and each block is discussed as follows:

A. Preprocessing

In the preliminary stage of segmentation the presence of darker and brighter areas obtained by variation in illumination leads to misinterpretation of such noises as lesion region [10]. Hence to classify and demarcate these two regions from each other, correction factor based algorithms are required as a preprocessing step. Multi-Scale Retinex (MSR) is used for improving the contrast of images with a numerous number of brightness, i.e., in an image with mix of shadow balanced with highlight provides the same image but makes all image layers greyer, since the ratio of current value to the average R component is substituted in place of each and every pixel. The major motive is to partition the dynamic range- compression features of MSR from color-constancy component. Following this the dynamic range compression is carried out to change image luminance with the hue of each pixel being unchanged.

B. Texture distinctiveness

The TDLS algorithm involves two major steps [9]: i. learning the sparse texture followed by calculation of TD metric to determine the difference of a texture distribution compared with the rest. ii. Classification of the image as skin or lesion using TD metric calculated from sparse texture with different texture patterns. Such models require only a negligible number of representations similar to patches for characterizing an entire image and permits to efficiently store the image and computation of algorithms. Optimization of problem is one of the many ways to clustering or formulates the features of images.

C. Representative texture distributions

The implemented algorithm makes use of statistical information with advantages to model both local as well as global texture characteristics for which a local texture vector of all pixels are obtained. The N ×M pixels with illumination correction covering a neighborhood of pixel size 'n' and 's' being the location of (x, y) of pixel. The vector is represented by n × n × a with padding of borders for the image [11]. Similarly for multiple channels, the vector is framed by concatenating tA,s subsequent to all channels. Let us assume for an instance, three channels {R,G,B} for each pixel and their corresponding texture vectors tR,s, tG,s, and tB,s, are extracted after concatenation such that ts = [tR,s, tG,s, tB,s]. After extraction, N ×M vectors with each vector of size n × n × a is given by the following condition:

$$T = \{tsj \mid 1 \le j \le N \times M\} \ldots\ldots\ldots (3)$$

With all essential vectors extracted and local and global characteristics being captured from an image are determined using representative texture distributions. The k th representative texture distribution is defined as Tr k by which the computational complexity and memory requirements are reduced as below:

$$T = \{T\ T\ 1\ k\ K\ K\} \ldots\ldots\ldots (4)$$

The k^{th} texture distribution in θk is characterized by all required set of parameters. Mixture model representation of input image is obtained by texture distributions. Texture distribution is particularly chosen to increase or extend the log-likelihood. Unsupervised clustering algorithm is used in order to predict the representative texture distributions corresponding to each of its associated distribution. The set Ck comprises texture vector associated with the same set of texture distributions.

D. Td metric

As distinction between two classes is of prime concern computation numerous texture distributions belonging to same class is carried out. With the frequency of occurrence that mean of one function being the mean of other also similarity between two texture distributions are to be measured defined by lj,k. The gross spread of lesion using texture due to color variegation along with patterns found in skin lesions is analyzed. The probability of distinctiveness is given by dj,k. The dissimilarity in texture distribution Tr j is given by Dj. The metric in [12] measures the expected distinctiveness using the probability of occurrence P(Tr k |I) for every pixel associated with Tr k. P(Tr k |I) is calculated using histogram.

Published By:
Blue Eyes Intelligence Engineering
and Sciences Publication (BEIESP)

The texture distinctiveness suffers from major setback that the difference between one skin texture distributions from the remaining is very negligible. To increase the textural distinctiveness metric, lesion texture distributions with dissimilar features from other skin are extracted.

E. Region classification

Following the previous step, TDLS algorithm for tracing and classifying the lesion regions based on the sparse texture distributions along with its associated TD metric is carried out. After over segmentation, the result is split into a more regions, with each classified independently from normal region is to refine the segmented lesion as a post processing step.

E.1 Initial Regions

The key reason behind initial region classification is for robustness of noise. The statistical region merging [13] is used for processing the image in RGB color space. The major pros of using the SRM algorithm are for tracing the pixel location, simplicity and to be computationally efficient.

Sorting and a Merging are two major steps involved in SRM algorithm to sort pixels for determining its order then merging pixels based on their similarity and is derived by a four- connected graph with its neighbors respectively. The sorting is done both along horizontal and vertical neighboring pixels depending on its number. The merging of two regions is determined based on pixel intensities and also difference between average pixel intensity for each channels.

A tunable parameter Q is set to 128 to change the likelihood of two merged regions. In order to decrease number of regions along with edges of the segments in photograph is merged into a single function. The regions nearest to the edges are likely to be under the portion of the normal skin class.

E.2 Distinctiveness-based Segment Classification

After performing over segmentation, each region must be classified based on afore- mentioned criterion [14]. Depending on the value of each element in y being 1 or 0, the classification results in corresponding region. The threshold is denoted by τ with boundary of decision. The two classes are classified by the textural distinctiveness metric DR based on the TD

$$y(R) = \{1, if DR \ (lesion); 0, normal \quad (5)$$

The parameter 'D' is calibrated for each texture distribution based on the similarity probability with other texture distributions. The determined information is to be combined with the contents regional TD metric and DR for every region.

E.3 Segmentation Refinement

The post-processing steps are applied to redefine the regions with morphological dilation and region selection with filling holes and smoothened border. The amount and shape of expansion of the binary mask is carried out by a structuring element with a radius of 5 pixels during which the small regions are eliminated and the largest pixels are grouped under lesion class.

F. NEURAL NETWORK

The neurons are trained with patterns along with its weight in a way similar to brain classification. The XYZ regions of each and every pixel are learnt from set of segmented images using neural network. The output response is that it produces 1 for lesion and 0 for normal skin [15]. The output of TDLS algorithm being a binary image the brighter and darker pixels associates to lesion and normal skin respectively but still the output is not accurate owing to thresholding. Hence the classification based on neural network is found to be comparatively more accurate.

IV. SIMULATION RESULTS AND ANALYSIS

The GLCM features for a set of samples are tabulated in the table below:

PARAMETERS	ACTINIC KERATOSIS	BASAL CELL CARCINOMA	MELANOMA	NORMAL SKIN
Co	0.0962	1.8579	0.9335	5.0565
Cr	0.9956	0.9000	0.9509	0.6974
Ee	0.5549	0.5844	0.5932	0.5665
Ho	0.9983	0.9668	0.9833	0.9097

Table No.1 Comparison of GLCM Parameter for Sample 1

PARAMETERS	ACTINIC KERATOSIS	BASAL CELL CARCINOMA	MELANOMA	NORMAL SKIN
Co	0.7855	0.4193	0.6693	3.1544
Cr	0.9613	0.9803	0.9678	0.8367
Ee	0.5703	0.5564	0.5620	0.5456
Ho	0.9860	0.9925	0.9880	0.9437

Table No.2 Comparison of GLCM Parameter for Sample 2

PARAMETERS	ACTINIC KERATOSIS	BASAL CELL CARCINOMA	MELANOMA	NORMAL SKIN
Co	5.1197	0.8431	0.8015	0.9414
Cr	0.6932	0.9597	0.9608	0.9555
Ee	0.5658	0.5565	0.5661	0.5493
Ho	0.9086	0.9849	0.9857	0.9832

Table No.3 Comparison of GLCM Parameter for Sample 3

PARAMETERS	ACTINIC KERATOSIS	BASAL CELL CARCINOMA	MELANOMA
Co	2.3262	0.4567	0.6929
Cr	0.8812	0.9782	0.9672
Ee	0.5552	0.5637	0.5547
Ho	0.9585	0.9918	0.9876

Table No.4 Comparison of GLCM Parameter for Sample 4

In Fig.3, the pre-processed and segmented images are tabulated. Sample 1 is a digital camera image obtained from patient's leg, Sample 2 is a digital camera image obtained from patient's chin, Sample 3 is a digital camera image obtained from patient's hand, and Sample 4 is a digital camera image obtained from patient's shoulder. The image samples obtained from various parts of patients are pre-processed since it is affected due to illumination effects. Hence illumination effects are corrected using multi Scale Retinex and the corrected images are converted into XYZ component.

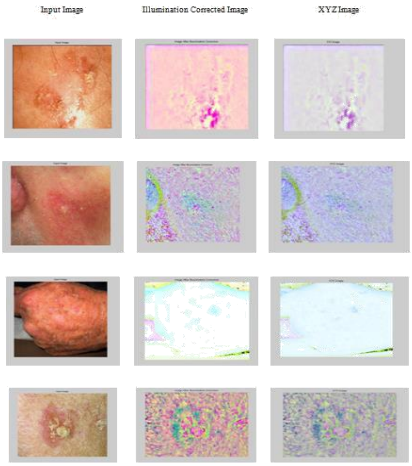

Fig.3 Tabulation of Segmentation of Actinic Keratosis

Published By:
Blue Eyes Intelligence Engineering
and Sciences Publication (BEIESP)

In Fig.4, the XYZ images are feed into K-Means clustering, where it is classified as Actinic keratosis based on the values obtained from GLCM features given in table 1-4 of samples used. In Fig.5, the pre-processed and segmented images are tabulated. Sample 1 is a digital camera image obtained from patient's nose, Sample 2 is a digital camera image obtained from patient's arm, Sample 3 is a digital camera image obtained from patient's hand.The image samples obtained from various parts of patients are pre-processed since it is affected due to illumination effects

Hence illumination effects are corrected using multi Scale Retinex and the corrected images are converted into XYZ component.

In Fig.6, the XYZ images are feed into K-Means clustering, where it is classified as Basal Cell Carcinoma based on the values obtained from GLCM features given in table 1-4 of samples used. In table no 1, the pre-processed and segmented images are tabulated. Sample 1 is a digital camera image obtained from patient's leg, Sample 2 is a digital camera image obtained from patient's arm, Sample 3 is a digital camera image obtained from patient's hand, Sample 4 is a digital camera image obtained from patient's shoulder. The image samples obtained from various parts of patients are pre-processed since it is affected due to illumination effects. Hence illumination effects are corrected using Multi Scale Retinex and the corrected images are converted into XYZ component. In table no 2, the XYZ images are feed into K-Means clustering, where it is classified as Melanoma based on the values obtained from GLCM features given in table 1-4 of samples used.

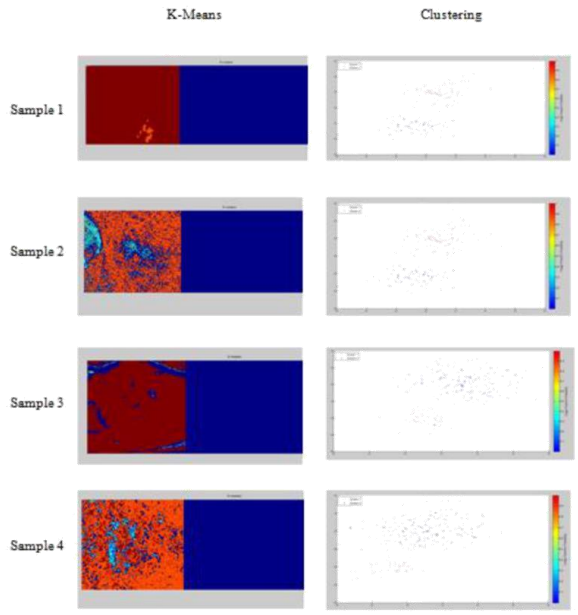

Fig.4 Tabulation of Clustering of Actinic Keratosis

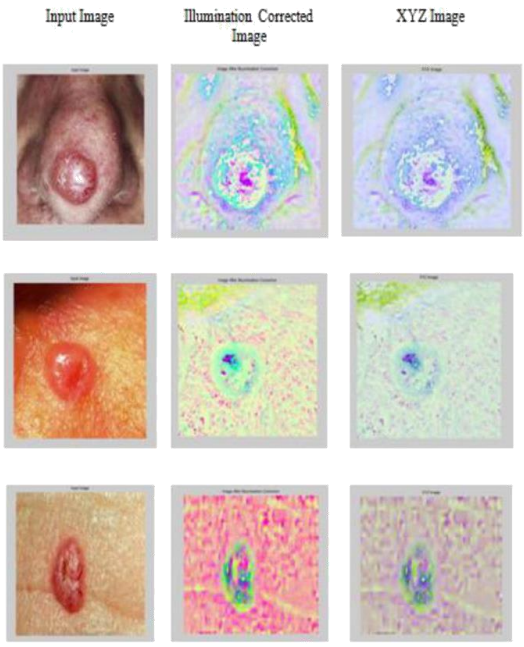

Fig.5 Tabulation of Segmentation of Basal Cell Carcinoma

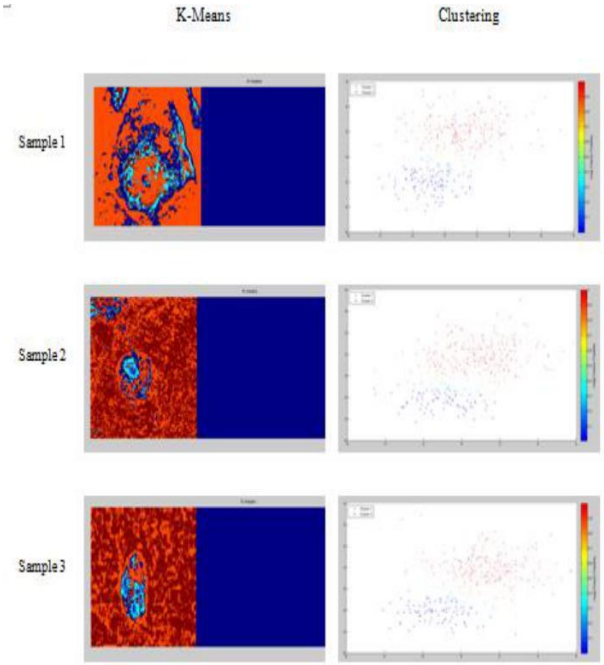

Fig.6 Tabulation of Clustering of Basal Cell Carcinoma

Published By:
Blue Eyes Intelligence Engineering and Sciences Publication (BEIESP)

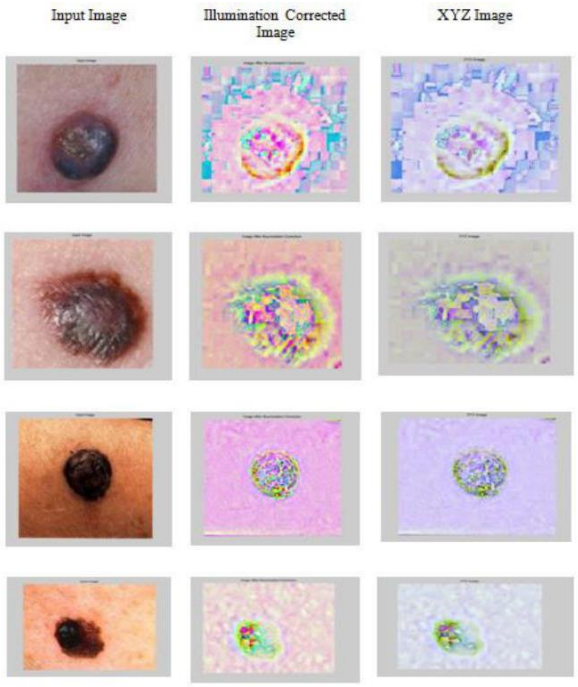

Fig.7 Tabulation of Segmented melanoma

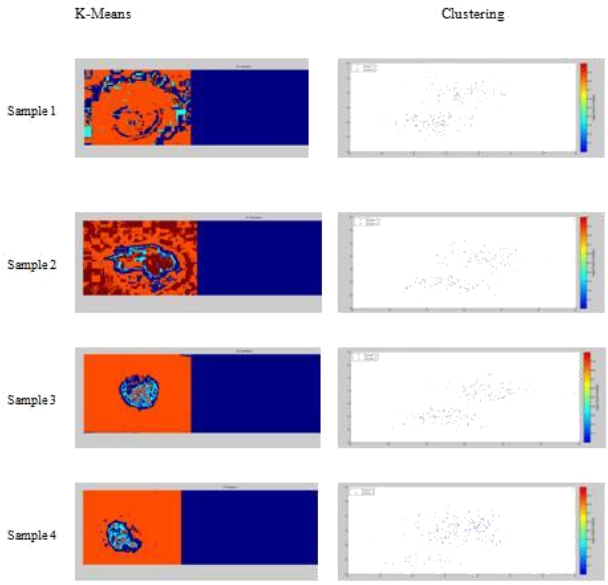

Fig.8 Tabulation of Clustering melanoma

In table no 3, the pre-processed and segmented images are tabulated. Sample 1 is a digital camera image obtained from patient's leg, Sample 2 is a digital camera image obtained from patient's hand, Sample 3 is a digital camera image obtained from patient's neck, Sample 4 is a digital camera image obtained from patient's shoulder. The image samples obtained from various parts of patients are pre-processed since it is affected due to illumination effects

Hence illumination effects are corrected using Multi Scale Retinex and the corrected images are converted into XYZ component. In table no 4, the XYZ images are feed into K-Means clustering, where it is classified as Normal Skin based on the values obtained from GLCM features given in table 1-4 of samples used.

V. CONCLUSION

Segmentation algorithm for lesion from normal region using the concept of neural network is validated on certain features of texture distinctiveness. The image is then divided into smaller regions for classification based on TD mapping. Skin region will have low distinctiveness when compared to the normal region. The learning or training is obtained from the pixels of segmented images through neural net work. Any deviation in the segmented output is corrected by a factor to achieve higher accuracy. A larger data is collected for simulation from MIT database of around 120 and annotated. The simulations prove that the proposed technique can perform segmentation of image over precise range of quality.

REFERENCES

1. Wong, A. ; Scharcanski ; Fieguth, P., 'Automatic Skin Lesion Segmentation via Iterative Stochastic Region Merging', Information Technology in Biomedicine, IEEE Transactions on, vo1.15, no.6, pp. 929,936, Nov. 2011
2. G. Di Leo, A. Paolillo, P. Sommella, and C. Liguori, 'An improved procedure for the automatic detection of dermoscopic structures in digital elm images of skin lesions', Proc. 2008 IEEE Comput. Soc. VECIMS, 2008, pp. 190–194.
3. J. Glaister, R. Amelard, A. Wong, and D. A. Clausi, 'MSIM: Multi-stage illumination modeling of dermatological photographs for illumination corrected skin lesion analyses, IEEE Transactions. vol. 60, no. 7,pp. 1873–1883, Jul. 2013.
4. C. Scharfenberger, A. Wong, K. Fergani, J. S. Zelek, and D. A. Clausi, 'Statistical textural distinctiveness for salient region detection in natural images', Proc. IEEE Conf. Jun. 2013
5. I S Akila and Sumathi V, 'Detection of Melanoma Skin Cancer using Segmentation and Classification Algorithms', IJCA Proceedings on National Conference on Information and Communication Technologies NCICT 2015(2):1-4, September 2015.
6. Pablo G. Cavalcanti, Jacob Scharcanski, 'Automated prescreening of pigmented skin lesions using standard cameras', Computerized medical imaging and graphics 35, pp.481-491, Feb 2011.
7. S.Hwang and M. E. Celebi, 'Texture segmentation of dermoscopy images using Gabor filters and g-means clustering', in Proc. Int. Conf.Image Process., Comput. Vision, Pattern Recog, Jul. 2010, pp. 882 886
8. M. Emre Celebi; Hitoshi Iyatomi; Gerald Schaefer; William V Stoecker, 'Lesion border detection in dermoscopy images', Computerized medical imaging and graphics 33, pp. 148-153, 2009
9. M. Sheha, M. S. Mabrouk, and A. Sharawy',Automatic detection of melanoma skin cancer using texture analysis' Int. J. Comput. Appl., vol. 42, no. 20, pp. 22–26, Mar. 2012.
10. Cavalcanti, P. G. Yari, Y. Scharcanski, J. 'Pigmented skin lesion segmentation on macroscopic images', Image and Vision Computing New Zealand (IVCNZ), 2010 25th International Conference of, vol., no., pp.1,7, 8-9 Nov. 2010
11. Sarrafzade, Baygi, M. H. M. ; Ghassemi, P., 'Skin lesion detection in dermoscopy images using wavelet transform and morphology operations', Biomedical Engineering (lCBME), 2010 17th Iranian Conference of, vol., no., pp. l, 4, 3-4 Nov. 2010

Published By:
Blue Eyes Intelligence Engineering and Sciences Publication (BEIESP)

12. S.Hwang and M. E. Celebi, 'Texture segmentation of dermoscopy images using Gabor filters and g-means clustering', in Proc. Int. Conf.Image Process., Comput. Vision, Pattern Recog, Jul. 2010, pp. 882 886
13. Richard Nock and F. Nielsen',Statistical region merging', IEEE Transactions. vol. 26, no. 11, pp. 1452–1458, Nov 2004
14. Trabelsi, 0.; Tlig, L. ; Sayadi, M. ; Fnaiech, F., 'Skin disease analysis and tracking based on image segmentation', Electrical Engineering and Software Applications (lCEESA), 2013 International Conference on, vol., no., pp.1,7, 21-23 March 2013
15. L. Xu, M. Jackowski, A. Goshtasby, D. Roseman, S. Bines,C.Yu, A. Dhawan, A. Huntley', Segmentation of skin cancer images' Image and Vision Computing 17 (1999)